Numerical Simulation of 3-D Film Blowing Process Under Thermal and Crystallinity Effects

Hatice Mercan[1,2] , Patrick D. Anderson[1], and Gerrit W. M. Peters[1]

[1] Eindhoven University of Technology, the Netherlands
[2] Yıldız Technical University, Turkey

ABSTRACT

The unsteady, axisymmetric 3-D film blowing flow of a polymer melt is studied numerically with thermal and crystallization effects. The mass, momentum and energy balance equations with constitutive and crystallinity equations are solved sequentially using Galerkin finite element discretization with updated movements of mesh and material.

INTRODUCTION

The polymer films are mostly produced by film blowing process. After extrusion, the polymer melt is stretched in radial direction by cooling air injected through the centre of the die, and in axial direction by the nip rolls. Due to crystallization, extension of the polymer melt in both the radial and down-stream directions stops at the frost line. This process is used extensively with polyethylene and polypropylene. In this study the 3-D film blowing process is modelled numerically for a LLDPE. Since the pioneering study of Pearson and Petrie[1-3] the numerical studies in the literature for film blowing process modeled blown films as a surface with mechanical properties of a membrane due to small bubble thickness. In these studies the computational domain reduced to a 1-D curve[1-11]. With these assumptions governing equations are related to the geometry of the film through kinematic relations and reduced to a set of highly-nonlinear ordinary differential equations. However this approach has many drawbacks: it is not possible to model the flow inside the die, the changes through the film thickness cannot be calculated and the stress boundary conditions at the die exit are not accurate. In this study we enlarged the computational domain further so that the tubular die is partially included, and solved for balance equations without any simplifications and minimized assumptions. The model presented in this study is solved numerically in 3-D axisymmetric space with a Finite Element code. The free surfaces are modeled using the Arbitrary Lagrangian Eulerian (ALE) formulation, thus the mesh movements with the material is captured. The governing equations are integrated in time sequentially with Explicit Euler method. The constitutive relations and the momentum balance are handled with a semi-implicit technique. Discrete Elastic-Viscoelastic Stress Split Method, Log-conformation representation and Streamline-Upwind Petrov Galerkin techniques are employed for stabilization purposes.

MATHEMATICAL FORMULATION

Figure 1 schematically shows the flow domain, boundary conditions and the mesh on which the balance equations are solved sequentially with the Galerkin finite element method. The annular die thickness is 1mm (R_O-R_i) the length of the film is 100mm.

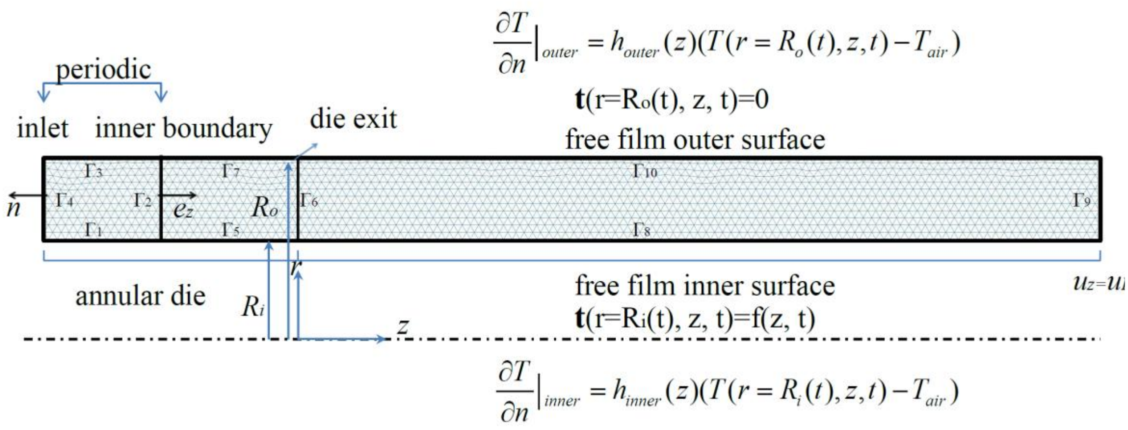

Figure 1. Geometry of the blown film, annular die and the boundary conditions

The die length is 20 mm. The traction-free conditions are applied on free film surfaces Γ_8 and Γ_{10}. No-slip boundary condition is applied on the die walls; Γ_1, Γ_5, Γ_3 and Γ_7. The constant temperature boundary is applied on the die walls and robin type of boundary condition is applied on free film surfaces and on boundary Γ_9 insulation boundary condition is applied. The convection heat transfer coefficients, h_{inner} and h_{outer}, the traction force $\mathbf{t}$ and the cooling air temperature T_{air}, are modified for the 3-D axisymmetric case.

The mass and momentum balance is given by

$$\nabla \cdot \mathbf{u} = \mathbf{0} \tag{1}$$
$$\nabla p - \nabla \cdot \boldsymbol{\tau} = \mathbf{0} \tag{2}$$

where $\mathbf{u}$ is the velocity vector, p is the pressure, $\boldsymbol{\tau}$ is the polymer extra stress tensor. eXtendend Pom-Pom (XPP) model is adopted as the constitutive relation for the polymer stresses. This viscoelastic constitutive model is successfully used to model fiber spinning, which is an extensional deformation process as well[12]. In terms of confirmation tensor $\mathbf{c}$, the XPP model reads:

$$\frac{\partial \mathbf{c}}{\partial t} + \mathbf{u} \cdot \nabla \mathbf{c} - (\nabla \mathbf{u})^{\mathrm{T}} \cdot \mathbf{c} - \mathbf{c} \cdot \nabla \mathbf{u} + \mathbf{f}(\mathbf{c}) = 0 \tag{3}$$

with

$$\mathbf{f}(\mathbf{c}) = \frac{2}{\lambda_s} \exp[\nu(\Lambda - 1)] \left(1 - \frac{3}{\operatorname{tr} \mathbf{c}}\right) \mathbf{c} + \frac{1}{\lambda_b}\left(\frac{3\mathbf{c}}{\operatorname{tr} \mathbf{c}} - 1\right). \tag{4}$$

where Λ is the tube stretch $\Lambda = \sqrt{\operatorname{tr} \mathbf{c}}$, λ_b is the relaxation time of the backbone tube orientation, λ_s is the relaxation time of the backbone tube stretch and the parameter ν is defined as $\nu = 2/q$ where q is the number of the arms at both ends of the backbone. In this study, we set $\lambda_b/\lambda_s=2$, and q=5.

Polymer extra stress tensor, for the XPP model, is given by

$$\boldsymbol{\tau} = \mathrm{G}(\mathbf{c} - \mathbf{I}) \tag{5}$$

Where modulus defined as $\mathrm{G} = \eta/\lambda_b$, η is the zero shear rate viscosity and $\mathbf{I}$ is the unit tensor. Logarithm of conformation tensor transformation is used to improve the numerical stability of the problem thus the constitutive relation in equation (3) has the following form:

$$\frac{\partial \mathbf{s}}{\partial t} + \mathbf{u} \cdot \nabla \mathbf{s} - \mathrm{g}((\nabla \mathbf{u})^{\mathrm{T}}, \mathbf{s}) = 0. \tag{6}$$

where log conformation equation $\mathbf{s} = \log(\mathbf{c})$ and back substitution $\mathbf{c} = \exp(\mathbf{s})$. For more details about the Log - Conformation Representation please see Van der Walt[12]. The movement of the free film surfaces are described by a height function H(z,t), which is initially defined by Keunings[14] and later applied to extrudate swell model by Choi[15] and fiber spinning by Van der Walt[12]. The unsteady kinematic relation for the height function in axial and radial direction is given by

$$\frac{\partial H}{\partial t} + u_{z,FS}\frac{\partial H}{\partial z} = u_{r,FS} \qquad (7)$$

where $u_{z,FS}$ and $u_{r,FS}$ are the axial and radial velocity components at the free surfaces, respectively. These equations are solved for obtaining both inner and outer free surface movements. The Arbitrary Lagrangian- Eulerian (ALE) formulation is used to maintain the adaptation of the free surfaces and the motion of the flow domain[12]. The initial and boundary conditions should be defined for t=0 and on the boundaries of the flow domain. The flow in the annular die is modelled as presented in Bogaerds et al.[14]. Between inlet and the inner boundary, periodic boundary conditions are applied, as shown in Figure 1. The die walls are imposed to no-slip boundary conditions. The free film surfaces are imposed to traction-free boundary conditions. The nip roll velocity is imposed at the end of the film. The initial conditions for the free surface film radii are set equal to the inner and outer die radii. The initial condition for the stress over the flow field is imposed over the conformation tensor, **c**(r,z,t=0)=1.

The energy balance equation reads;

$$\rho c_p\frac{DT}{Dt} = k\nabla^2 T + \rho\chi_\infty \Delta H\frac{D\chi}{Dt} + \boldsymbol{\sigma}:\mathbf{D} \qquad (8)$$

where $\frac{D}{Dt}$ denotes the material derivative, ρ is density, c_p is the heat capacity, k is the thermal conductivity, χ_∞ is the final crystallinity, ΔH is the heat fusion, **σ** is the stress tensor and **D** is the rate of strain tensor. The Drichlet type boundary condition is used in the die walls and Robin type boundary condition is used at the free film surfaces. The convective heat transfer coefficient is defined as a seventh order polynomial with constant coefficients. The proposed heat transfer coefficient used in this study is obtained by integrating the heat transfer coefficient used in the study of Doufas[11] along the film, see Fig. 2.

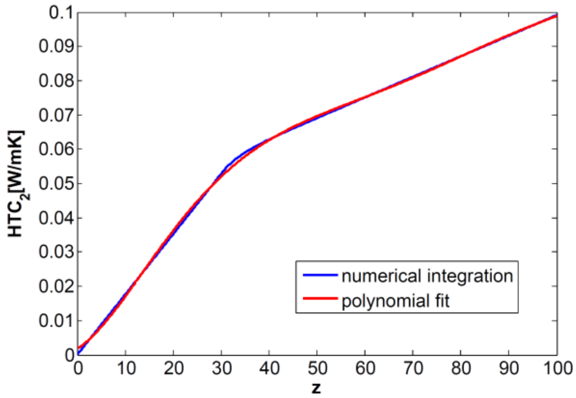

Figure 2. Fitting of the heat transfer coefficient for the free film surfaces, numerical integration of the coefficient in the literature[11], the 7th order polynomial fit used in this study

The Schneider rate equations are used to calculate the volume fraction of the crystalline structure due to cooling. At an undisturbed volume the kinematic relations for the crystal structure development for length density, surface density and volume density are as follows:

$$\begin{aligned} \dot{\phi}_3 &= 8\pi N \\ \dot{\phi}_2 &= G\phi_3 \\ \dot{\phi}_1 &= G\phi_2 \\ \dot{\phi}_0 &= G\phi_1 \end{aligned} \qquad (9)$$

where G is the crystal growth rate and N is the nucleation rate. The flow induced component of the kinematic relations structure development for length density, surface density and volume density are as follows:

$$\begin{aligned} \dot{\psi}_3 &= 8\pi N'_f \\ \dot{\psi}_2 &= G_n N_f L \\ \dot{\psi}_1 &= G_n\psi_2 \\ \dot{\psi}_0 &= G_n\psi_1 \end{aligned} \qquad (10)$$

where N'_f is the flow induced nucleation rate, G_n is the flow induced crystal growth rate, L is the length of shish per unit volume. The total space filling is calculated with Kolmogorov-Avrami model as follows:

$$-\ln(1-\chi) = \psi_0 + \phi_0 \qquad (11)$$

Initial condition for the space filling is taken equal to 10^{-5}everywhere in the flow domain.

RESULTS

In this section the results of the 3-D model is presented. First the temperature and crystallinity effects are investigated and the results are compared with the results in the literature under similar process conditions.

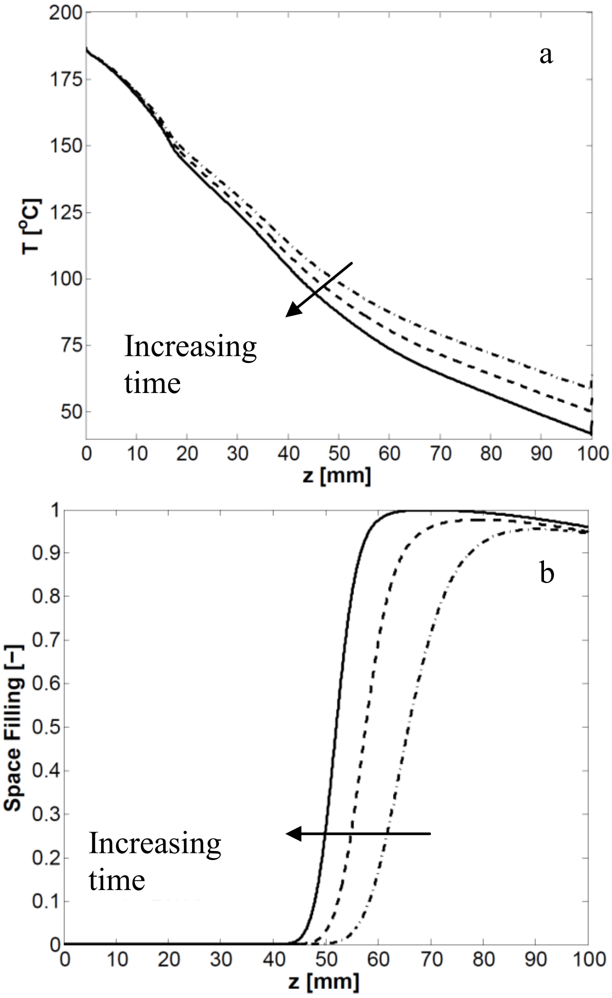

Figure 3. (a) Temperature distribution evolution along the outer film surface (b) space filling distribution evolution along the outer film surface, D_R=10, ΔP=0.0015 XPP model

In Figure 3, the temperature and space filling distributions are shown for advancing time. The corresponding bubble shape is shown in Figure 4. The freeze line for this case is observed around z=65mm. The changes along the thickness around freeze line z=65, is shown in Figures 5.

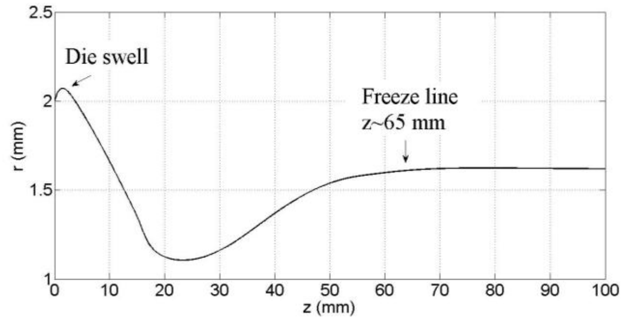

Figure 4. Bubble shape, D_R=10, ΔP=0.0015 XPP model

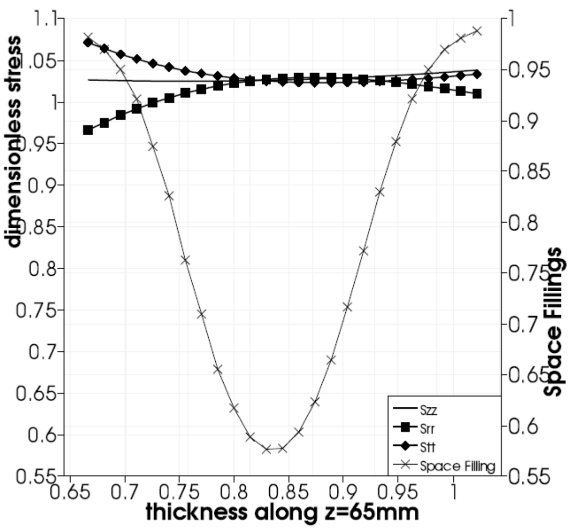

Figure 5. Dimensionless stresses and space filling distributions along the thickness at z=65mm, D_R=10, ΔP=0.0015 XPP model

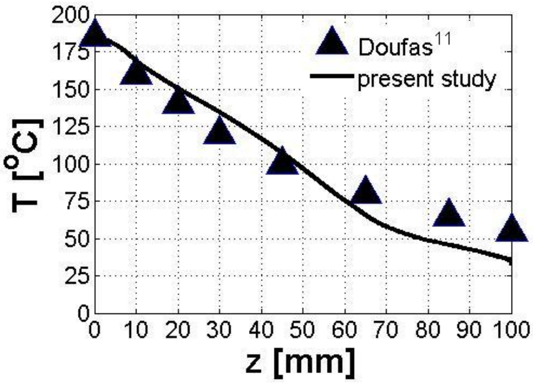

Figure 6. Comparison of the film temperature with the experimental result in the literature[11], D_R=10, ΔP=0.0015 XPP model

The available heat transfer coefficients in the literature are mostly for steady state representations where the cooling occurs through the machine direction. However the present formulation is unsteady and the cooling takes place through the free surfaces. The heat transfer coefficients along the free surfaces are obtained using the available experimental and numerical studies in the literature. By means of the new boundary conditions the converged results for non-isothermal case is shown in Fig. 1 to 5 and the comparison with the literature is shown in Fig.6.

A new and efficient numerical method is developed for unsteady film blowing process with inclusion of die region. Steady results are successfully obtained for moderate draw ratio and low pressure difference. This algorithm will be valuable tool to analyze the rheological processes with free surfaces.

REFERENCES

1. Pearson J.R.A, Petrie C.J.S. (1970), "The flow of a tubular film Part1 Formal mathematical representation", *J. Fluid Mech.*, **40**, 1-19.

2. Pearson J.R.A, Petrie C.J.S. (1970), "The flow of a tubular film Part 2 Interpretation of the model and discussion of solutions", *J. Fluid Mech.* **42**, 609-625.

3. Petrie C.J.S. (1975), "A comparison of theoretical predictions with published experimental measurements on blow film process", *AIChE J,* **21**, 275.

4. Han C. D., Park J. Y. (1975), "Studies on blown film extrusion: II. Analysis of the deformation and heat transfer process", *J. of Appl. Polymer Sci*. **19**, 3257.

5. Wagner M. H. (1978), "A rheologic-thermodynamic process, model of the film-blowing process", *Rheologica Acta*, **15**, 40.

6. Kanai T., White J.L. (1984), "Kinematics, dynamics and stability of the tubular film extrusion of various polyethylenes", *Polymer Eng. Sci.* **24**, 1185.

7. Cao, B.P., Sweeney P., Campbell A.G. (1989), "Simultaneous surface and bulk temperature measurement of polyethylene during film blowing", *SPE ANTEC* **35**.

8. Muslet I.A, Kamal M.R. (2004), "Computer simulation of the film blowing process incorporating crystallization and viscoelasticity", *I.J. Rheol* **55(2)**, 257-271.

9. Sarafrazi S., Sharif F. (2008), "Non-isothermal simulation of the film blowing process using multi-mode eXtended Pom-Pom model", *International Polymer Processing XXIII* **1**, 30-37.

10. Lee S. J., Jung H. W., Hyun J. C. (2011) "Transient solutions of non-linear dynamics in film blowing process accompanied by on-line crystallization", *Journal of Rheology* **48(3)**, 525-550.

11. A.K. Doufas (2014) "A microstructural flow-induced crystallization model for film blowing: validation with experimental data", *Rheologica Acta* **53**, 269-293.

12. C. van der Walt, Hulsen M.A., Bogaerds A.C.B., Anderson P.D. (2013), "Transient modeling of fiber spinning with filament pull-out", *Journal of Non-Newtonian Fluid Mechanics* **208-209** 72-87.

13. M.A. Hulsen, Fattal R., Kupferman R. (2005) "Flow of viscoelastic fluids past a cylinder at high Weissenberg number: Stabilized simulations using matrix logarithm", *Journal of Non-Newtonian Fluid Mechanics* **127**, 27-39.

14. A.C.B. Bogaerds, Grillet A.M., Peters G.W.M., Baaijens F.P.T. (2002) "Stability analysis of polymer shear flows using the Extended Pom-Pom constitutive equations", *Journal of Non-Newtonian Fluid Mechanics* **108**, 187-208.